Plant Physiology®

Plant Physiology, 2025, **197**, kiaf111
https://doi.org/10.1093/plphys/kiaf111
Advance access publication 21 March 2025
Research Report

Membranous translation platforms in the chloroplast of *Chlamydomonas reinhardtii*

Yi Sun,[1,†,‡] Shiva Bakhtiari,[1,†] Melissa Valente-Paterno,[1,§] Heng Jiang,[2] William Zerges[1,*]

[1]Department of Biology, Concordia University, 7141 Sherbrooke W, Montreal, Quebec H4B 1R6, Canada
[2]Centre for Biological Applications of Mass Spectrometry, Concordia University, 7141 Sherbrooke W, Montreal, Quebec H4B 1R6, Canada
*Author for correspondence: william.zerges@concordia.ca
†These authors contributed equally to this work.
‡Present address: Department of Biology, University of Oxford, South Parks Road, Oxford OX1 3RB, UK.
§Present address: Department of Anatomy and Cell Biology, McGill University, 3640 University, Montreal, Quebec H3A 0C7, Canada.
The author responsible for distribution of materials integral to the findings presented in this article in accordance with the policy described in the Instructions for Authors (https://academic.oup.com/plphys/pages/General-Instructions) is William Zerges (william.zerges@concordia.ca).

Abstract

A small genome in chloroplasts encodes many of the polypeptide subunits of the photosynthetic electron transport complexes embedded in the membranes of thylakoid vesicles in the chloroplast stroma and synthesized by ribosomes of the bacterial-like genetic system of this semiautonomous organelle. While thylakoid membranes (TMs) are sites of translation, evidence in the unicellular alga *Chlamydomonas reinhardtii* supports translation on noncanonical membranes in a discrete translation zone in the chloroplast. To characterize the membranous platforms for translation and the biogenesis of TMs, we profiled membranes during chloroplast development, using the *yellow-in-the-dark1* mutant, and carried out proteomic analyses on 2 membrane types proposed previously to support translation in the chloroplast of *C. reinhardtii*: "low-density membrane" (LDM) and "chloroplast translation membrane" (CTM). The results support the roles of LDM and CTM in the preliminary and ongoing stages of translation, respectively. Proteomics, immunoprecipitation, and transmission electron microscopy results support connections of these membranous platforms and a chloroplast envelope domain bound by cytoplasmic ribosomes. Our results contribute to a model of photosynthesis complex biogenesis in a spatiotemporal "assembly line" involving LDM and CTM as sequential stages leading to photosynthetic TMs.

Introduction

Chloroplasts have some 3,000 proteins for their biogenesis, homeostasis, and specialized functions, such as photosynthesis. Most chloroplast proteins are encoded by the nuclear genome, synthesized in the cytosol by 80S ribosomes, and then imported across the dual membranes of the chloroplast envelope (Rochaix 2023). Other chloroplast proteins are encoded by the chloroplast genome and synthesized by the bacterial-type 70S ribosomes of this semiautonomous organelle (Sun and Zerges 2015). Among these are integral membrane subunits of the photosynthetic electron transport (PET) complexes and ATP synthase, which are embedded in the membranes of the thylakoid vesicles within the chloroplast (Ostermeier et al. 2024). These subunits are integrated into a membrane during their synthesis, i.e. co-translationally. While it is widely believed that translation for de novo photosystem biogenesis occurs on thylakoid membranes (TMs), recent evidence supports roles for specialized membranous translation platforms in cyanobacteria and chloroplasts (Schottkowski et al. 2012; Chotewutmontri and Barkan 2024; Ostermeier et al. 2024). In the unicellular alga Chlamydomonas (*Chlamydomonas reinhardtii*) within the chloroplast, the "translation zone" (T-zone) is specialized in the synthesis and assembly of photosystem subunits and chlorophyll and is more discretely localized than the TM throughout the chloroplast (Sun et al. 2019). The candidate membranes of the T-zone are "low-density membrane" (LDM) and "chloroplast translation membrane" (CTM) (Zerges and Rochaix 1998; Schottkowski et al. 2012). These roles are based on the cofractionation of LDM and CTM with a few marker proteins of translation by chloroplast ribosomes and photosystem biogenesis (Zerges and Rochaix 1998; Schottkowski et al. 2012).

Here, we report comprehensive evidence of the roles of LDM and CTM as platforms for distinct phases of TM biogenesis. This evidence includes changes in the relative levels of LDM, CTM, and TM before, during, and after chloroplast differentiation and their compositions with respect to proteins of TM biogenesis and photosynthesis. Finally, we provide evidence that LDM and CTM participate in the spatial coordination of the translation systems of the chloroplast and cytosol for the localized synthesis and targeting of chloroplast proteins (Billakurthi and Loudya 2024; Sun et al. 2024).

Results

Membranes with chloroplast ribosomes change during chloroplast development

We profiled the relative levels of LDM, CTM, and TM before, during, and after chloroplast differentiation in *yellow-in-the-dark1* (*y1*) cells (Ohad et al. 1967; Malnoe et al. 1988). When *y1* is cultured in the dark (on acetate instead of photosynthesis), these "dark-*y1* cells"

Received January 13, 2025. Accepted February 9, 2025.

have an undifferentiated plastid lacking photosystems and TM resulting from their deficiency for the chlorophyll biosynthetic enzyme light-independent protochlorophyllide-oxido-reductase and a requirement for chlorophyll in the biogenesis of the photosystems and TM (Cahoon and Timko 2000). Upon illumination, dark-*y1* cells commence chlorophyll biosynthesis, using a light-dependent protochlorophyllide-oxido-reductase, and over the subsequent 12 h in the light carry out enhanced rates of translation in the chloroplast for photosystem and TM biogenesis (Malnoe et al. 1988; Sun et al. 2019). Thus, dark-*y1* cells are poised for high levels of chloroplast translation. After 2 h of illumination, "2h-*y1* cells" undergo high levels of chloroplast translation for photosystem biogenesis. After 16 h of illumination, "16h-*y1* cells" are phenotypically wild-type and undergo translation for cellular growth and homeostasis.

We compared LDM, CTM, and TM in dark-*y1*, 2h-*y1*, and 16h-*y1* cells by fractionating their fragmented membranes by buoyant density and then testing the fractions for relevant marker proteins. Post-greening, 16h-*y1* cells yielded abundant TM, seen as a band with the highest levels of PSI and PSII (Fig. 1, A and D , F4). 16h-*y1* cells also yielded CTM in F5 to F7, which were detected by the presence of markers for the 30S and 50S subunits of the chloroplast ribosome, low PSI and PSII levels, and higher buoyant density relative to TM (Fig. 1D) (Schottkowski et al. 2012). Dark-*y1* cells yielded an abundant membrane seen as a discrete yellow band (Fig. 1, A and B, F5). This band contained CTM because it had the highest levels of 30S and 50S chloroplast ribosomal subunits and was denser than the TM in the gradient of 16h-*y1* cell membranes (Fig. 1, A, B, and D) (Schottkowski et al. 2012). This fraction also had trace amounts of the PSI and PSII subunits that accumulate under these conditions, consistent with the proposed role of CTM in TM protein synthesis. Chloroplast ribosomes on CTM were likely translating because dark-*y1* cells synthesize photosystem subunits, albeit at lower rates than do 2h-*y1* cells (Sun et al. 2019).

LDM was prominent in dark-*y1* cells (Fig. 1B, F2 to F4) (Sun et al. 2019). This LDM had a higher ratio of the 30S to 50S chloroplast ribosomal subunits compared with CTM (Fig. 1, compare the 30S/50S marker ratios of LDM in 1B, F2 to F4, versus of CTM in 1D, F5 and F6, or of TM in 1D, F4). This feature supports an early role because the initiation phase of translation involves the 30S subunit but not the 50S subunit (Laursen et al. 2005). This is also supported by the appearance of the 50S subunit marker protein in the low-density fractions during the first 2 h of greening, e.g. for the assembly of the 70S ribosome as translation enhances (Fig. 1, compare F2 and F3 in 1B versus in 1C). High rates of chloroplast translation in greening 2h-*y1* cells correlated with a prominence of membranes with both chloroplast ribosome subunits and the translation activator RNA-binding protein of 40 kDa (RBP40) (Fig. 1C) (Schwarz et al. 2007). These results reveal that the activation of chloroplast translation during *y1* greening increases CTM abundance and buoyant density range.

Proteomic results support the roles of LDM and CTM as platforms for chloroplast protein synthesis and assembly

We carried out proteomic analyses of LDM and CTM to characterize their functions. LDM was isolated from wild-type cells

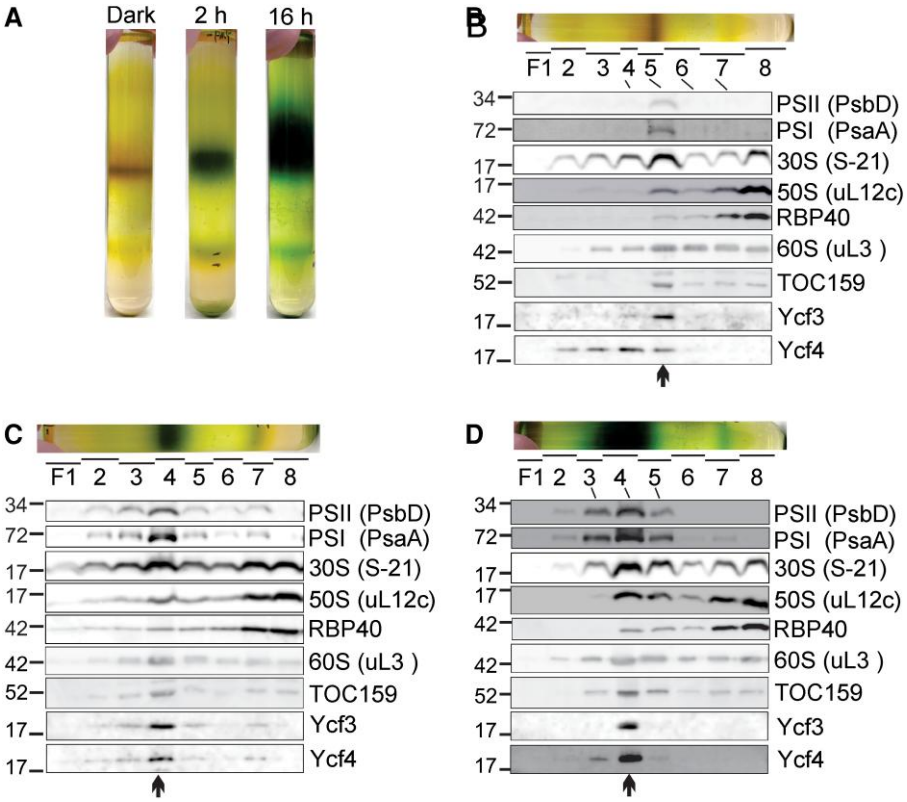

Figure 1. Density profiles of chloroplast membranes before, during, and after TM biogenesis in *y1* greening. **A)** Sucrose density gradient ultracentrifugation fractionated membranes from dark-*y1* cells, 2h-*y1* cells, and 16h-*y1* cells. During isopycnic ultracentrifugation, membranes floated from a dense sucrose cushion (F8) to equilibrate in the gradient by buoyant density and were then collected as F1 to F7. Immunoblot analyses of fractions from (**B**) dark-*y1* cells, (**C**) 2h-*y1* cells, and (**D**) 16h-*y1* cells revealed levels of markers for the photosystems (PsbD and PsaA) and biogenesis: the chloroplast ribosome subunits of 30S (S-21) and 50S (uL12c), the translation activator RBP40, cytoplasmic ribosomes (uL3), the TOC complex (TOC159), and the PSI assembly factors (Ycf3 and Ycf4). **B** to **D)** Arrows point to fractions with the highest levels of cytoplasmic and chloroplast ribosome markers (see text). **B** to **D)** Lanes were loaded with equal proportions of the total rather than by equal protein mass amounts. Molecular mass markers are in kDa.

(Zerges and Rochaix 1998). Immunoblot results confirmed that TM had higher levels of PSI and PSII markers whereas LDM had higher levels of markers for translation and chloroplast biogenesis: the chloroplast ribosome (S-21), a protein of the TOC chloroplast protein import translocon (Toc159), RBP40, and an enzyme in the chlorophyll branch of the tetrapyrrole biosynthetic pathway (PORA) (Fig. 2A). LDM preparations had higher levels of the AtpB subunit of the chloroplast ATP synthase, which was unexpected for a complex that functions in conjunction with PET and is believed to be only in TM (Hahn et al. 2018).

Our proteomic analyses of LDM included comparisons to TM with a quantitative approach based on differential metabolic labeling with stable N isotopes (Gouw et al. 2010). To characterize CTM, we carried out label-free proteomic analysis of the sucrose density gradient F5 of dark-y1 cell membranes (Fig. 1B). Two independent biological replicates were carried out from separate cultures for each membrane type. Biogenic proteins were assorted into the categories seen in Fig. 2, C and D. Identified proteins in LDM and CTM are listed in Tables 1 and 2, respectively. Photosynthetic proteins were categorized by their function in either PET, LHC, or ATP synthase. PET proteins were more numerous in TM (51 proteins) than in LDM (30) or CTM (27) (Tables 1 and 2). The representations of the protein categories in LDM, CTM, and TM were compared as the sums of all protein

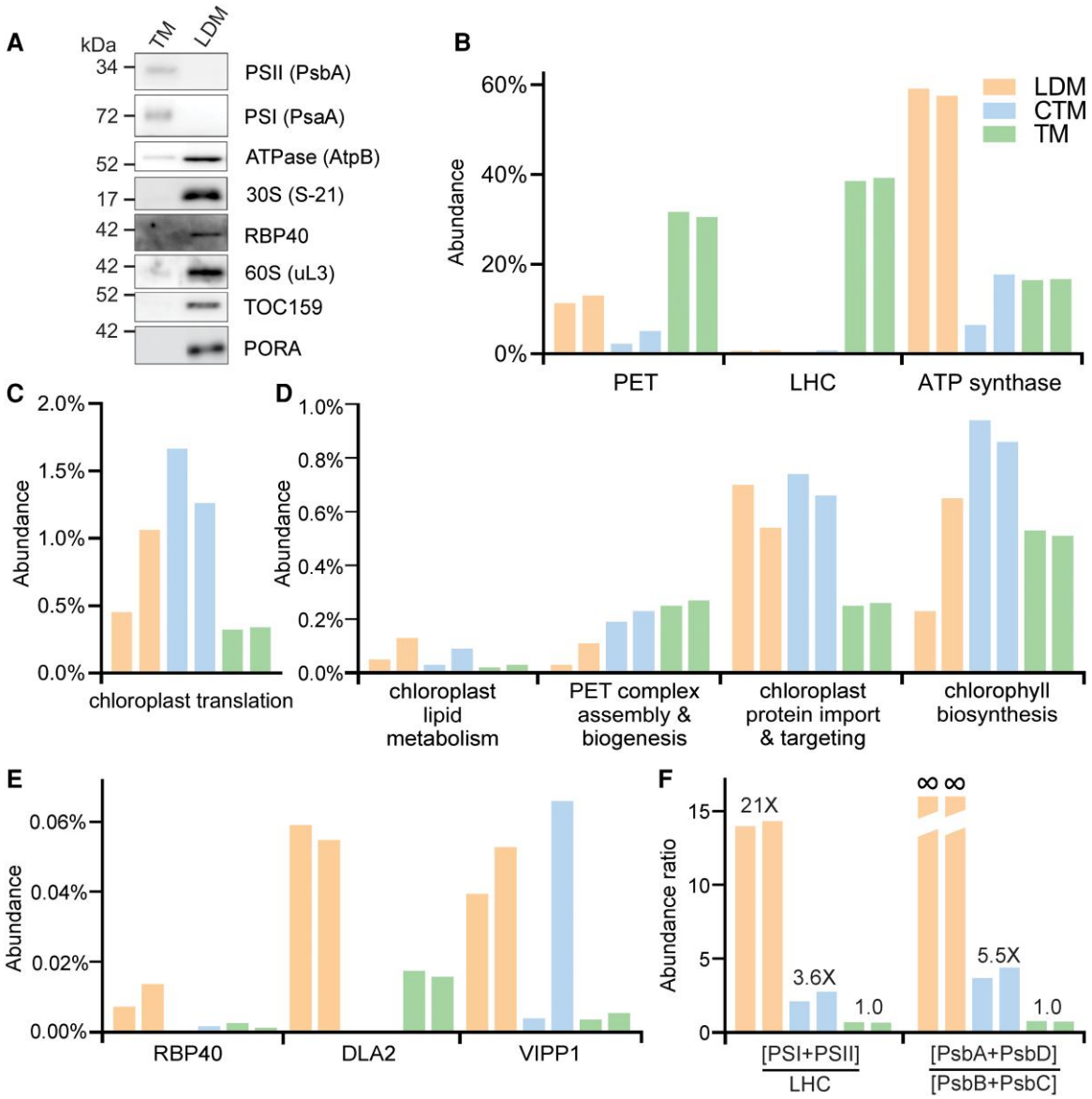

Figure 2. Proteomic analyses of LDM and CTM support their roles as translation platforms for TM biogenesis. **A)** Immunoblot analyses revealed the relative levels in LDM and TM of marker proteins for PSII (PsbA), PSI (PsaA), the chloroplast ATP synthase (AtpB), the chloroplast translation (S-21 and RBP40), the cytoplasmic ribosome (uL3), chlorophyll biosynthesis (PORA), and chloroplast protein import (TOC159). Molecular mass markers are in kDa. Lanes were loaded with equal protein mass amounts. **B** to **F)** Abundances of proteins in each category are indicated by bar heights. Dual bars represent the biological replicate trials 1 and 2. For lists of identified proteins in each category, see Tables 1 and 2 and Supplementary Data File 1. **B** to **E)** Bar heights indicate the representations by the functional categories, as the sum of the abundances of the proteins therein as the percent total abundances of all proteins in the sample. Categories were (**B**) photosynthetic complexes of PET, LHC, and ATP synthase, (**C**) chloroplast translation, (**D**) chloroplast lipid metabolism, PET complex assembly, chloroplast protein import and targeting, and chlorophyll biosynthesis (**E**) RBP40, RBP63/DLA2, VIPP1, and (**F**) abundance ratios of photosystem proteins to LHC proteins and PsbA and PsbD to PsbB and PsbC. Values above each bar pair represent fold difference relative to TM. The 2 left-most bars for LDM were assigned ∞ because these ratios cannot be calculated with PsbB and PsbC abundance values of zero in the denominator.

Table 1. The LDM proteome

Biogenesis; protein and lipid metabolism
Protein import and targeting: CDJ1, TIC62, TIC110.
PET complex assembly: HCF136, PSB27, YCF3.
TM lipid bilayer biogenesis: VIPP1, PLAP9, PLAP10.
Biogenesis; chlorophyll biosynthesis
Mg-chelatase (CHLD, CHLH1), Mg-protoporphyrin IX *S*-adenosyl methionine *O*-methyl transferase (CHLM), Mg-protoporphyrin IX monomethyl ester [oxidative] cyclase 1 (CRD1), Mg-protoporphyrin IX monomethyl ester oxidative cyclase 2 (CTH1), 3,8-divinyl protochlorophyllide a 8-vinyl reductase (DVR1), protochlorophyllide reductase, chloroplastic, light-dependent (PORA), protoporphyrinogen oxidase (Ppx1), chloroplast phytoene desaturase (PDS1), Geranylgeranyl reductase (CHLP/GGR).
Biogenesis; chloroplast translation
30S: bS1c, uS4c, uS5c, uS7c, uS9c, uS11c, uS13c, uS14c, uS15c, bS16c, uS17c, bS18c, uS19c, bS20c, PSRP-1, PSRP-3.
50S: uL1c, uL3c, uL4c, uL6c, bL9c, uL11c, bL12c, uL13c, uL14c, uL15c, bL17c, uL18c, uL23c, uL24c, bL28c, bL31c.
Regulators: Rap38, RB38/RBP40, DLA2/RBP63.
Biogenesis; cytoplasmic translation
40S: eS1 (S3a), uS2 (Sa), uS3 (S3), eS4 (S4), uS4 (S9), uS5 (S2), eS6 (S6), uS7 (S5), eS7 (S7), uS8 (S15A), eS8 (S8), uS9 (S16), eS10 (S10), uS11 (S14), eS12 (S12), uS13 (S18), eS17 (S17), uS19 (S15), eS19 (S19), eS25 (S25), eS26 (S26), eS28 (S28), eS31 (S27a).
60S: uL1 (L10a), uL3 (L3), uL4 (L4), uL5 (L11), eL6 (L6), uL6 (L9), uL10 (P0), uL11 (L12), eL13 (L13), uL13 (L13a), eL14 (L14), uL15 (L27a), eL18 (L18), uL18 (L5), eL19 (L19), eL21 (L21), uL22 (L17), uL23 (L23a), eL24 (L24), uL24 (L26), eL27 (L27), eL28 (L28), uL29 (L35), uL30 (L7), eL34 (L34), P2.
Photosynthetic electron transport and ATP synthase
Photosynthetic electron transport: PETC, PETH, PETO, PsaD, PSAF, PSAG, PSAH, PSAK, PSAN, PsbA, PsbD, PSBO, PSBP1, PSBQ, PSBR, FNR1, LhcII-1.3, LhcII-4, Lhcb4, LHCA3, LHCA7, LHCA9, Lhcb3, lhcb5, LHCBM4, LhcI-3, LhcI-5, LhcII-3, LHCSR1, LHCSR3.2.
ATP synthase: AtpA, AtpB, ATPC, ATPD, AtpE, ATPG, AtpF.
Predicted/unknown (Supplementary Data File 1)
Other (Supplementary Data File 1)

The proteins identified in LDM are listed according to their known functions in chloroplast biogenesis or photosynthesis. Ribosomal protein names are provided according to the revised nomenclature, and the previous names for cytoplasmic ribosomal proteins are given in parentheses (Ban et al. 2014). The older names are not provided for chloroplast ribosomal proteins because the numbers therein did not change (Willmund et al. 2022). For additional information, see Supplementary Data File 1.

Table 2. The CTM proteome

Biogenesis; protein and lipid metabolism
Protein import and targeting: OEP80/TOC75-V, Ycf1/ORF1995, TOC34, TOC75, CPLD5, TIC20, TIC21, TIC22, TIC40, TIC62, TIC110, CDJ1, FTSHi1, HCF106/TATB, SECY1, SRP43, SRP54L, SECA1, TPP1.
PET complex assembly: ycf3, ycf4, HCF136, ALB3.1, ALB3.2, PSB27, PIR1, PSBP4, CCB1, CCB2, CCB4, CCS1.
TM lipid bilayer biogenesis: VIPP1, TGD2, MGD1, PLAP2, CPLD55.
Biogenesis; chlorophyll biosynthesis
Protoporphyrinogen oxidase (Ppx1), Geranylgeranyl reductase (CHLP), Mg-protoporphyrin IX chelatase (CHLD), Mg-protoporphyrin IX *S*-adenosyl methionine *O*-methyl transferase (CHLM), Mg-protoporphyrin IX monomethyl ester oxidative cyclase 1 (CRD1), Mg-protoporphyrin IX monomethyl ester oxidative cyclase 2 (CTH1), Protochlorophyllide reductase, light-dependent (PORA), Protochlorophyllide reductase, light-independent (ChlL, ChlB), chloroplast Flu-like protein long form (FLU), Chloroplast phytoene desaturase (PDS1), 3,8-divinyl protochlorophyllide a 8-vinyl reductase (DVR1), light-independent protochlorophyllide reductase subunit N (ChlN), uroporphyrinogen decarboxylase (UROD3).
Biogenesis; chloroplast translation
30S: bS1c, uS2c, uS3c, uS4c, uS5c, bS6c, uS7c, uS8c, uS9c, uS10c, uS12c, uS13c, uS14c, uS15c, bS16c, uS17c, bS18c, uS19c, bS20c, bS21c, PSRP-1, PSRP-3.
50S: uL1c, uL2c, bL34c, uL3c, uL4c, uL5c, uL6c, bL9c, uL10c, bL12c, uL13c, uL14c, uL15c, uL16c, uL18c, bL19c, bL20c, uL23c, uL24c, bL28c.
Other: Rap38/CSP41b, PETs, PABP/RB47, tufA/EF-Tu, RB38/RBP40, RBP63/DLA2.
Biogenesis; 80S cytoplasmic translation
40S: eS1 (S3a), uS2 (Sa), uS3 (S3), eS4 (S4), uS4 (S9), uS5 (S2), eS6 (S6), uS7 (S5), eS7 (S7), uS8 (S15A), eS8 (S8), uS9 (S16), eS10 (S10), uS10 (S20), eS11 (S11), uS11 (S14), eS12 (S12), uS12 (S23), uS13 (S18), uS14 (S29), uS15 (S13), eS17 (S17), uS19 (S15), eS19 (S19), eS21 (S21), eS24 (S24), eS25 (S25), eS26 (S26), eS27 (S27), eS28 (S28), eS30 (S30), eS31 (S27a).
60S: uL1 (L10a), uL2 (L8), uL3 (L3), uL4 (L4), uL5 (L11), eL6 (L6), uL6 (L9), L7a (eL8), uL10 (P0), uL11 (L12), eL13 (L13), uL13 (L13a), eL14 (L14), uL14 (L23), eL15 (L15), uL15 (L27a), uL16 (L10), eL18 (L18), uL18 (L5), eL19 (L19), eL20 (L18a), eL21 (L21), uL22 (L17), eL22 (L22), uL23 (L23a), eL24 (L24), uL24 (L26), eL27 (L27), eL28 (L28), uL29 (L35), eL30 (L30), uL30 (L7), eL31 (L31), eL32 (L32), eL33 (L35a), eL34 (L34), eL36 (L36), eL37 (L37), eL38 (L38), eL39 (L39), eL43 (L37a), eL44 (L44), P1, P2.
Other: UTP30/RSL1D1, EEF1, EF-3, EFG2, EFG5, EIF1A, EIF2Ab, EIF3A, EIF3B, EIF3C, EIF3D, EIF3E, EIF3F, EIF3G, EIF3H, EIF3I, EIF3K, EIF3L, EIF4A3/FAL1, EIF4A-like, EIF6A.
Photosynthetic electron transport and ATP synthase
PS I: PSAF, PSAH, FNR1.
PS II: PsbA, PsbB, PsbC, PsbD, PSBO, PsbE, PsbH, PSBR, PSBP1, PSBQ
Lhcb4, LHCBM1, LHCBM2, LHCBM3, LHCBM5, LHCBM6.
Cytochrome b6/f: PetA, PetB, PETC, PetD, PETE, PETO, TEF5.
ATP synthase: AtpA, AtpB, ATPC, ATPD, ATPE, ATPF, ATPG, AtpI.
Predicted/unknown (Supplementary Data File 1)
Other (Supplementary Data File 1)

Ribosomal protein names are according to the revised nomenclature with the previous names for cytoplasmic ribosomal proteins given in parentheses (Ban et al. 2014). For additional information, see Table 1 legend and Supplementary Data File 1.

abundance values in each category expressed as a percentage of the sum of all protein abundances in the sample (Fig. 2, B to E). PET and LHC proteins were most abundant in TM, their known location (Fig. 2B). The results support the biogenic roles of LDM and CTM (Discussion) and the high abundance of ATP synthase in LDM.

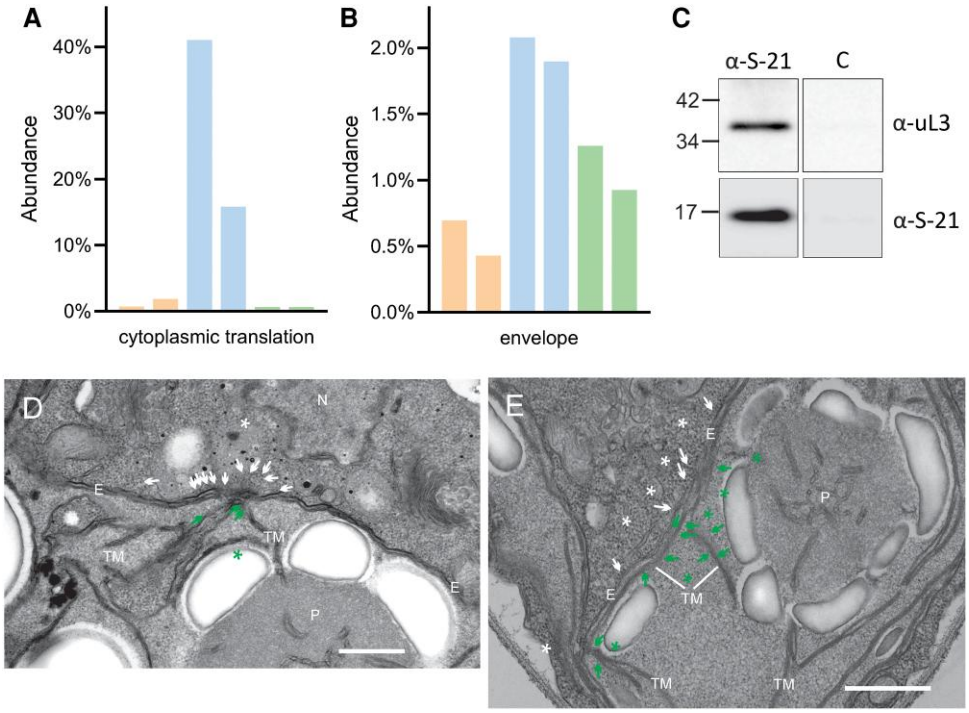

Figure 3. Evidence of physical connections between membranous translation platforms for cytoplasmic ribosomes and chloroplast ribosomes. **A** and **B)** Abundance (y-axis) is the sum of protein abundances in the category as the percentage of the total protein abundance in the sample. Each pair of bars represents the results of the 2 independent biological replicate experiments. Trials 1 and 2 are the left and right bars, respectively. The protein function categories are (**A**) cytoplasmic ribosomal proteins and (**B**) envelope proteins. Bar colors are: LDM, orange; CTM, blue; TM, green. **C)** Membranes with the cytoplasmic ribosome marker protein uL3 were coimmunoprecipitated with membranes with the chloroplast ribosome marker S-21. In the negative control ("C"), preimmune serum from the rabbit that generated αS-21 was used instead of the latter. Molecular mass markers are in kDa. **D)** A TEM image of chloroplast of a 2h-*y1* cell shows a connection between the chloroplast envelope (labeled "E") and TMs, which is indicated by equidistant white and green asterisks in the cytoplasm and the chloroplast, respectively. Structures resembling cytoplasmic ribosomes and polysomes are indicated with white arrows, and chloroplast ribosomes and polysomes with green arrows. **E)** A TEM image from the chloroplast of a wild-type cell undergoing rapid TM biogenesis at ZT2 in the diel cycle with the same labeling as in **A**. See Supplementary Fig. S1 for these images without labeling and images of each entire cell indicating the chloroplast and cropped region and additional image sets. N, nucleus; P, pyrenoid. Bars = 500 nm.

Associations between membranes with cytoplasmic ribosomes and chloroplast ribosomes

Translation by chloroplast ribosomes in the T-zone is aligned with translation by cytoplasmic ribosomes on a domain of the chloroplast envelope where the latter synthesize proteins encoded by the nuclear genome for localized import into the chloroplast (Sun et al. 2024). This spatial alignment of the dual translation systems might involve associations between their membranous translation platforms. Indeed, proteins of both systems and envelope proteins were more abundant in CTM than in LDM or TM (Figs. 2C and 3, A and B). We observed cofractionation of membranes with the cytoplasmic and chloroplast ribosomal proteins and the TOC translocon marker protein TOC159 (Fig. 1, B to D, see arrows below each panel). Moreover, the membranes with these translation and import markers decreased together in buoyant density during greening (Fig. 1, B to D, F5 in dark-*y1* cells and F4 in 2h- and 16h-*y1* cells). A cytoplasmic ribosome marker (uL3) was coimmunoprecipitated with a chloroplast ribosomal protein (S-21) (Fig. 3C). Finally, we observed contact sites between the ends of thylakoid lamellae and the inner envelope membrane in the T-zone in transmission electron microscopy (TEM) images of 2h-*y1* cells and wild-type cells undergoing rapid TM biogenesis (Fig. 3, D and E, Supplementary Fig. S1). Near these contact sites, structures resembling cytoplasmic ribosomes and chloroplast ribosomes, mostly in polysomes, were near or on the outer envelope membrane and thylakoid lamellae, respectively.

Discussion

The roles of LDM and CTM as membranous platforms for translation and photosystem assembly are supported by their having proteins in these processes, their prominence during chloroplast differentiation, and differences in their compositions of photosynthesis proteins relative to TM. For example, LDM and CTM were enriched in proteins of the chloroplast ribosome and chloroplast protein import and targeting, and they had multiple proteins in chloroplast lipid metabolism and PET complex assembly and biogenesis (Fig. 2D, Tables 1 and 2, Supplementary Data File 1). Both CTM and LDM had enzymes in the biosynthesis of chlorophyll, which is the major photopigment in the PET system and binds to apo-proteins during or immediately after their synthesis (Fig. 2, C and D) (Minagawa and Takahashi 2004). That LDM and CTM had minor amounts of subunits of the photosystems and LHCs is consistent with their being both distinct from TM and platforms for the synthesis and assembly of these proteins (Fig. 2B). Similar evidence in cyanobacteria supports the plasma membrane as the location of photosystem assembly and the origin of TM (Smith and Howe 1993; Zak et al. 2001; Stengel et al. 2012; Ostermeier et al. 2024).

An early role of LDM in a spatiotemporal "assembly line" of TM biogenesis is supported by several results (Fig. 4). Dark-*y1* cells had more prominent LDM than did 2h-*y1* or 16h-*y1* cells and were poised for high levels of translation by chloroplast ribosomes (Fig. 1, B, C, and D) (Sun et al. 2019). The higher ratio of 30S to 50S

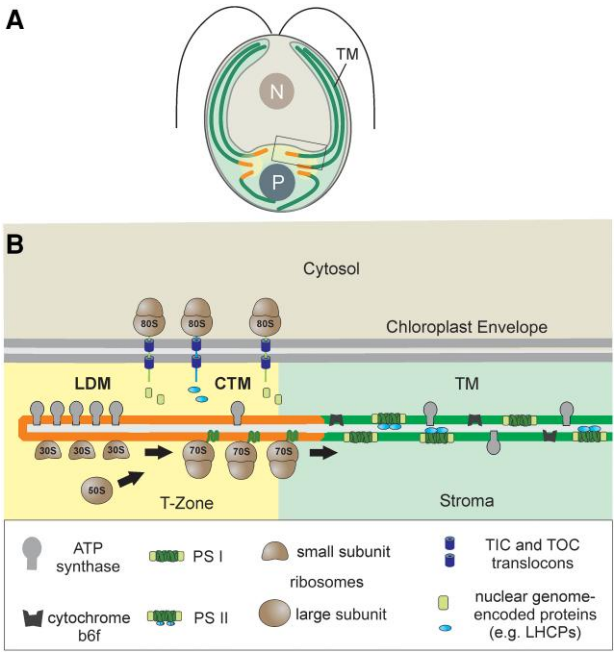

Figure 4. The model for the organization of LDM and CTM in the chloroplast. **A)** An illustration of a Chlamydomonas cell shows the nucleus (N), cytoplasm, and chloroplast (light green) with its T-zone (yellow), pyrenoid (P), thylakoid vesicles (dark green, TM), envelope (blue), and LDM and CTM (orange). The rectangular box shows the region illustrated in **B**. **B)** LDM is a platform for the preliminary stages of translation and photosystem biogenesis. On CTM, 70S ribosomes synthesize chloroplastic genome-encoded subunits of PSI and PSII for assembly. The resulting PSI and PSII reaction centers are bound by subunits expressed from the nuclear genome and imported by the protein translocons of the outer and inner chloroplast envelope membranes, TOC and TIC, respectively (purple cylinders) (Schottkowski et al. 2012). Newly assembled photosystems diffuse from CTM to TM throughout the chloroplast.

chloroplast ribosomal subunits in LDM, relative to CTM and TM, is consistent with a preferential role of LDM in the initiation phase of translation over the elongation phase (Laursen et al. 2005) (Fig. 1B). LDM was enriched in proteins required early in TM and photosystem biogenesis. Only 3 PET complex assembly factors were identified in LDM, of which 2 in the former have very early roles (HCF136 and YCF3), and compared to the 12 in CTM (Tables 1 and 2, Supplementary Data File 1) (Plucken et al. 2002; Nellaepalli et al. 2018). Only LDM had RBP63/DLA2 and RBP40, activators of translation initiation on the chloroplast mRNAs encoding the PSII reaction core subunits that are synthesized first in the PSII assembly pathway, PsbA and PsbD, respectively (Schwarz et al. 2007; Bohne et al. 2013; Choquet and Wollman 2023). Moreover, we identified PsbA and PsbD in LDM, but not PSII core subunits synthesized later, i.e. PsbB and PsbC (Fig. 2F, Supplementary Data File 1). A protein that functions very early in the biogenesis of the TM lipid bilayer, VIPP1, was more abundant in LDM than in TM (Fig. 2E) (Gupta et al. 2021). Finally, LDM had a ~20-fold higher abundance ratio of photosystem proteins to LHC proteins, compared to this ratio in TM (Fig. 2F), suggesting that photosystems had not yet assembled in LDM for their association with LHCs (Dreyfuss and Thornber 1994; Minagawa and Takahashi 2004). Abundances of proteins in chloroplast protein import and targeting were similar in LDM and CTM, and higher in each than in TM, consistent with the requirement for newly synthesized proteins throughout PET complex assembly (Fig. 2D).

In the model, the position of LDM at the termini of thylakoid lamella is supported by its enrichment in chloroplast ATP synthase proteins, a feature of the curvature domain at the ends of thylakoid lamellae in Arabidopsis (*Arabidopsis thaliana*) (Figs. 2, A and B and 4B) (Chotewutmontri and Barkan 2024). In mitochondria, ATP synthase has an early role in the curvature of the inner membrane to initiate the formation of cristae (Blum et al. 2019). Finally, LDM might support ATP synthase biogenesis, which occurs before photosystem biogenesis in the light phase of the diel cycle in Chlamydomonas and, hence, possibly in an early compartment of TM biogenesis (Zones et al. 2015; Sun et al. 2019).

We posit that LDM gives rise to CTM as it recruits the 50S subunit to join the 30S subunit thereby forming the 70S chloroplast ribosome (Fig. 4B). Accordingly, the 50S subunit and RBP40 appeared in the low-density fractions during the initial 2 h of *y1* greening (Fig. 1, B and C). The role of CTM as a platform for ongoing translation and photosystem assembly is also supported by its prominence in 2h-*y1* cells, correlating with the highest rates of translation for photosystem biogenesis of the 3 stages analyzed (Fig. 1C, F4 to F6) (Sun et al. 2019). As the synthesis of photosystem subunits is linked to their assembly and the binding to chlorophyll (Zoschke and Bock 2018), the enrichment of CTM in proteins in these categories supports it being a platform for PET complex biogenesis (Fig. 2D, Table 2). Enrichment of CTM in the PSI assembly factors Ycf3 and Ycf4 was also seen in immunoblot results (Fig. 1B, F4 and 1C, F5). Finally, CTM had ratios of photosystem proteins to LHC proteins and of early assembled PSII core subunits (PsbA and PsbD) to late assembled subunits (PsbB and PsbC) (see above) which were intermediate to these ratios in LDM and TM supporting the position of CTM between LDM and TM (Fig. 4B).

That TM had assembly factors and chloroplast ribosomes could reflect the possibility that membranes completing TM biogenesis acquire the density of TM, contamination of TM by CTM, or translation and assembly on mature TM, e.g. for PSII repair (Zoschke and Bock 2018).

In the model, newly synthesized PET complex subunits diffuse from LDM to CTM, where they assemble with each other and with LHCs, and then continue as assembled complexes to mature TM throughout the chloroplast (Fig. 4). Directionality is imposed by localized synthesis and assembly in LDM and CTM. The rate of lateral diffusion of complexes in TM (~0.5 μm/min, Kirchhoff et al. 2008) is sufficient for photosystems generated in the T-zone to populate the entire thylakoid network by diffusion over several microns in the ~5 h window of photosystem biogenesis in the cell cycle (Zones et al. 2015; Sun et al. 2019).

Our results of proteomics, immunoprecipitation, and TEM extend our understanding of the spatial coordination of the dual translation systems to the biochemical and ultrastructural levels (Figs. 2 and 3) (Sun et al. 2024). Contact sites, such as thylakoid convergence zones and invaginations of the inner envelope membrane have been proposed to be locations of TM biogenesis in Chlamydomonas (Engel et al. 2015; Ostermeier et al. 2024). Most of the contacts seen here involve thylakoid lamellae largely parallel to the envelope membrane, whereas those of convergence zones are closer to perpendicular (Fig. 3, D and E, Supplementary Fig. S1). In the cyanobacterium *Synechocystis* 6803, "thylakoid convergence tubes" have been proposed as a region for PSII biogenesis and are similar to the contact sites described here in that they are locations where TMs converge and are parallel to the plasma membrane, which is homologous to the inner envelope membrane, and are bound by ribosomes (Ostermeier et al. 2024). Evidence of a TM assembly line in Arabidopsis is supported by a lateral heterogeneity of TM in which

the earliest steps in photosystem biogenesis are localized to curvature domains at thylakoid termini, which are depleted of photosystems and thus analogous to LDM (Chotewutmontri and Barkan 2024). Later steps in Arabidopsis are localized to the neighboring "refined margin" domains, which could be analogous to CTM. Thus, the proposed spatiotemporal organization involving membranous translation platforms may be a conserved feature of TM biogenesis.

Materials and methods

Strains and culture conditions

All cultures were grown at 24 °C under a light intensity of 150 μE/m^2 s and with orbital shaking unless stated otherwise. Cells were collected by centrifugation (3,000 *g*, 5 min at RT). LDM was isolated from CC-400 (CW15, MT+) cultured in high salt minimal (HSM) (Harris 1989) with 1.0% (w/v) sorbitol. TEM was performed on 2h-*y1* cells (Sun et al. 2019). For differential quantitative mass spectrometry (MS) using metabolic labeling in the analysis of LDM versus TM, cultures were grown on a tris-acetate-phosphate (TAP) medium containing either [^{14}N]NH_4Cl (LDM) or [^{15}N]NH_4Cl (TM). *y1* (CC-1168) was cultured on a TAP medium in the dark and greening was induced by exposure to white light at 150 μE/m^2 s. Wild-type (CC-125) ZT2 cells of the diel cycle for TEM were obtained as described previously (Sun et al. 2019).

Membrane fractionation

y1 membranes for the density profiles in Fig. 1 and the proteomic analyses of CTM and TM were prepared as described previously (Schottkowski et al. 2012). The MS analyses were carried out on LDM purified as reported previously (Zerges and Rochaix 1998).

Immunoblot analysis

Proteins were transferred to PVDF (BIO-RAD) and reacted with primary and secondary antibodies as described previously (Sambrook and Russell 2001). The primary antibodies were: α-TOC159 (1:8,000) (Agrisera, AS07 239), α-AtpB (1:6,000), α-S-21 (1:3,000) (Randolph-Anderson et al. 1989), α-uL12c (1:10,000), α-uL3 (1:6,000), α-PsbA (1:5,000) (Agrisera, AS11 1786), α-PsbD (1:4,000) (Agrisera, AS06 146), α-PsaA (1:60,000), α-RBP40 (1:1,000), α-PORA (1:20,000), α-Ycf3 (1:3,000), and α-Ycf4 (1:3,000) (Supplementary Methods). The secondary antibody was horseradish peroxidase-conjugated goat anti-rabbit IgG antibody (KPL). Signals were detected using an ECL substrate (Thermo Fisher) with an Imager 600 (Amersham/GE).

Mass spectrometry (see Supplementary Methods)

Immunoprecipitation

Chloroplasts were isolated from CC-400 (CW15, MT+) cultured as described (Sun et al. 2024), and the pellet was resuspended in an ice-cold tris-potassium-magnesium (TKM) buffer [25 mM $MgCl_2$, 20 mM KCl, 10 mM Tricine-HCl pH 7.5, protease inhibitor cocktail for plants (Sigma-Aldrich)]. Chloroplasts were broken by 4 passes through an ice-chilled French Pressure Cell at 1,000 psi. The lysate was ultracentrifuged at 100,000×*g* for 1 h at 4 °C. The pellet was resuspended in an ice-cold TKM buffer as input. α-S-21 (1:1,000) or, as a negative control, preimmune serum from the same rabbit (1:1,000) was incubated with the input overnight at 4 °C with slow rotation. Dynabeads Protein A (Thermo Fisher) were prepared according to the manufacturer's protocol, incubated with the sample or control mixture at 4 °C for 2 h with rotation, washed according to the manufacturer's protocol, then resuspended in an SDS-PAGE loading buffer and incubated at 70 °C for 5 min.

TEM was carried out as described previously (Sun et al. 2019).

Accession numbers

Accession numbers can be found in Supplementary Data File 1.

Acknowledgments

The authors thank the Centre for Structural & Functional Genomics and the Centre for Biological Applications of Mass Spectrometry (Concordia University). For antibodies, the authors thank Elizabeth Harris (αAtpB and α-uL3), Jorg Nickelsen (αRBP40), Kevin Redding (αPsaA), Yuichiro Takahashi (α-Ycf3 and α-Ycf4), and Katrin Philippar and Prof. Jurgen Soll (α-PORA). For technical assistance and support, the authors thank Kelly Sears and Jeannie Mui and the Faculty for Electron Microscopy Research at McGill University.

Author contributions

Y.S., S.B., and W.Z. designed the research; Y.S., S.B., and M.V.-P. performed the research; Y.S., S.B., H.J., and W.Z. analyzed the data; Y.S. and W.Z. wrote the paper.

Supplementary data

The following materials are available in the online version of this article.

Supplementary Figure S1. TEM images support Fig. 3, D and E.
Supplementary Date File 1. Proteomic results.
Supplementary Methods.

Funding

This work was supported by the Natural Sciences and Engineering Research Council of Canada Grant (217566) to W.Z.

Conflict of interest statement. None declared.

Data availability

Data are available upon reasonable request. The mass spectrometry proteomics data have been deposited to the ProteomeXchange Consortium via the PRIDE partner repository with the dataset identifier PXD058102 (Perez-Riverol et al. 2022).

References

Ban N, Beckmann R, Cate JH, Dinman JD, Dragon F, Ellis SR, Lafontaine DL, Lindahl L, Liljas A, Lipton JM, *et al.* A new system for naming ribosomal proteins. *Curr Opin Struct Biol*. 2014:24:165–169. https://doi.org/10.1016/j.sbi.2014.01.002

Billakurthi K, Loudya N. Co-translational import of nuclear-encoded proteins into the chloroplast in *Chlamydomonas reinhardtii*. *Plant Physiol*. 2024:96(1):10–11. https://doi.org/10.1093/plphys/kiae310

Blum TB, Hahn A, Meier T, Davies KM, Kühlbrandt W. Dimers of mitochondrial ATP synthase induce membrane curvature and self-assemble into rows. *Proc Natl Acad Sci U S A*. 2019:116(10):4250–4255. https://doi.org/10.1073/pnas.1816556116

Bohne AV, Schwarz C, Schottkowski M, Lidschreiber M, Piotrowski M, Zerges W, Nickelsen J. Reciprocal regulation of protein synthesis and carbon metabolism for thylakoid membrane biogenesis. *PLoS Biol*. 2013:11(2):e1001482. https://doi.org/10.1371/journal.pbio.1001482

Cahoon AB, Timko MP. *yellow-in-the-dark* mutants of Chlamydomonas lack the CHLL subunit of light-independent protochlorophyllide reductase. *Plant Cell*. 2000:12(4):559–568. https://doi.org/10.1105/tpc.12.4.559

Choquet Y, Wollman F-A. Chapter 19: The assembly of photosynthetic proteins. In: Grossman AR, Wollman F-A, editors. *The Chlamydomonas sourcebook*. 3rd ed. London: Academic Press; 2023. p. 615–646.

Chotewutmontri P, Barkan A. Localization of proteins involved in the biogenesis and repair of the photosynthetic apparatus to thylakoid subdomains in Arabidopsis. *Plant Direct*. 2024:8(11):e70008. https://doi.org/10.1002/pld3.70008

Dreyfuss BW, Thornber JP. Organization of the light-harvesting complex of photosystem I and its assembly during plastid development. *Plant Physiol*. 1994:106(3):841–848. https://doi.org/10.1104/pp.106.3.841

Engel BD, Schaffer M, Kuhn Cuellar L, Villa E, Plitzko JM, Baumeister W. Native architecture of the Chlamydomonas chloroplast revealed by in situ cryo-electron tomography. *eLife*. 2015:4:1–29. https://doi.org/10.7554/eLife.04889

Gouw JW, Krijgsveld J, Heck AJ. Quantitative proteomics by metabolic labeling of model organisms. *Mol Cell Proteomics*. 2010:9:11–24. https://doi.org/10.1074/mcp.R900001-MCP200

Gupta TK, Klumpe S, Gries K, Heinz S, Wietrzynski W, Ohnishi N, Niemeyer J, Spaniol B, Schaffer M, Rast A, *et al.* Structural basis for VIPP1 oligomerization and maintenance of thylakoid membrane integrity. *Cell*. 2021:184(14):3643–3659.e23. https://doi.org/10.1016/j.cell.2021.05.011

Hahn A, Vonck J, Mills DJ, Meier T, Kühlbrandt W. Structure, mechanism, and regulation of the chloroplast ATP synthase. *Science*. 2018:360(6389):eaat4318. https://doi.org/10.1126/science.aat4318

Harris EH. *The Chlamydomonas sourcebook: a comprehensive guide to biology and laboratory use*. San Diego: Academic Press; 1989.

Kirchhoff H, Haferkamp S, Allen JF, Epstein DBA, Mullineaux CW. Protein diffusion and macromolecular crowding in thylakoid membranes. *Plant Physiol*. 2008:146(4):1571–1578. https://doi.org/10.1104/pp.107.115170

Laursen BS, Sorensen HP, Mortensen KK, Sperling-Petersen HU. Initiation of protein synthesis in bacteria. *Microbiol Mol Biol Rev*. 2005:69(1):101–123. https://doi.org/10.1128/MMBR.69.1.101-123.2005

Malnoe P, Mayfield SP, Rochaix JD. Comparative analysis of the biogenesis of photosystem II in the wild-type and Y-1 mutant of *Chlamydomonas reinhardtii*. *J Cell Biol*. 1988:106(3):609–616. https://doi.org/10.1083/jcb.106.3.609

Minagawa J, Takahashi Y. Structure, function and assembly of photosystem II and its light-harvesting proteins. *Photosynth Res*. 2004:82(3):241–263. https://doi.org/10.1007/s11120-004-2079-2

Nellaepalli S, Ozawa S-I, Kuroda H, Takahashi Y. The photosystem I assembly apparatus consisting of Ycf3–Y3IP1 and Ycf4 modules. *Nat Commun*. 2018:9(1):2439. https://doi.org/10.1038/s41467-018-04823-3

Ohad I, Siekevitz P, Palade GE. Biogenesis of chloroplast membranes. II. Plastid differentiation during greening of a dark-grown algal mutant (*Chlamydomonas reinhardi*). *J Cell Biol*. 1967:35(3):553–584. https://doi.org/10.1083/jcb.35.3.553

Ostermeier M, Garibay-Hernández A, Holzer VJC, Schroda M, Nickelsen J. Structure, biogenesis, and evolution of thylakoid membranes. *The Plant Cell* 2024;36:4014–4035. https://doi.org/10.1093/plcell/koae102

Perez-Riverol Y, Bai J, Bandla C, García-Seisdedos D, Hewapathirana S, Kamatchinathan S, Kundu DJ, Prakash A, Frericks-Zipper A, Eisenacher M, *et al.* The PRIDE database resources in 2022: a hub for mass spectrometry-based proteomics evidences. *Nucleic Acids Res*. 2022:50(D1):D543–D552. https://doi.org/10.1093/nar/gkab1038

Plucken H, Muller B, Grohmann D, Westhoff P, Eichacker LA. The HCF136 protein is essential for assembly of the photosystem II reaction center in *Arabidopsis thaliana*. *FEBS Lett*. 2002:532(1–2):85–90. https://doi.org/10.1016/S0014-5793(02)03634-7

Randolph-Anderson BL, Gillham NW, Boynton JE. Electrophoretic and immunological comparisons of chloroplast and prokaryotic ribosomal proteins reveal that certain families of large subunit proteins are evolutionarily conserved. *J Mol Evol*. 1989:29(1):68–88. https://doi.org/10.1007/BF02106183

Rochaix J-D. Historical overview. *The Chlamydomonas sourcebook*. 3rd ed. Vol 2. Amsterdam, Netherlands: Academic Press; 2023. p. 1–22.

Sambrook J, Russell DW. *Molecular cloning: a laboratory manual*. 3rd ed. Cold Spring Harbor (NY): Cold Spring Harbor Laboratory Press; 2001.

Schottkowski M, Peters M, Zhan Y, Rifai O, Zhang Y, Zerges W. Biogenic membranes of the chloroplast in *Chlamydomonas reinhardtii*. *Proc Natl Acad Sci U S A*. 2012:109(47):19286–19291. https://doi.org/10.1073/pnas.1209860109

Schwarz C, Elles I, Kortmann J, Piotrowski M, Nickelsen J. Synthesis of the D2 protein of photosystem II in *Chlamydomonas* is controlled by a high molecular mass complex containing the RNA stabilization factor Nac2 and the translational activator RBP40. *Plant Cell*. 2007:19(11):3627–3639. https://doi.org/10.1105/tpc.107.051722

Smith D, Howe CJ. The distribution of photosystem I and photosystem II polypeptides between the cytoplasmic and thylakoid membranes of cyanobacteria. *FEMS Microbiol Lett*. 1993:110(3):341–347. https://doi.org/10.1111/j.1574-6968.1993.tb06346.x

Stengel A, Gugel IL, Hilger D, Rengstl B, Jung H, Nickelsen J. Initial steps of photosystem II de novo assembly and preloading with manganese take place in biogenesis centers in Synechocystis. *Plant Cell*. 2012;24(2):660–675. https://doi.org/10.1105/tpc.111.093914

Sun Y, Bakhtiari S, Valente-Paterno M, Wu Y, Nishimura Y, Shen W, Law C, Dhaliwal J, Dai D, Bui KH, *et al.* Chloroplast biogenesis involves spatial coordination of nuclear and organellar gene expression in Chlamydomonas. *Plant Physiol*. 2024:196(1):112–123. https://doi.org/10.1093/plphys/kiae256

Sun Y, Valente-Paterno MI, Bakhtiari S, Law C, Zhan Y, Zerges W. Photosystem biogenesis is localized to the translation zone in the chloroplast of Chlamydomonas. *Plant Cell*. 2019;31(12):3057–3072. https://doi.org/10.1105/tpc.19.00263

Sun Y, Zerges W. Translational regulation in chloroplasts for development and homeostasis. *Biochim Biophys Acta*. 2015:1847(9):809–820. https://doi.org/10.1016/j.bbabio.2015.05.008

Willmund F, Hauser C, Zerges W. Translation and protein synthesis in the chloroplast. *The Chlamydomonas sourcebook*. 2022:2:467–508. https://doi.org/10.1016/B978-0-12-821430-5.00014-6

Zak E, Norling B, Maitra R, Huang F, Andersson B, Pakrasi HB. The initial steps of biogenesis of cyanobacterial photosystems occur in plasma membranes. *Proc Natl Acad Sci U S A*. 2001:98(23):13443–13448. https://doi.org/10.1073/pnas.241503898

Zerges W, Rochaix J-D. Low density membranes are associated with RNA-binding proteins and thylakoids in the chloroplast of *Chlamydomonas reinhardtii*. *J Cell Biol*. 1998:140(1):101–110. https://doi.org/10.1083/jcb.140.1.101

Zones JM, Blaby IK, Merchant SS, Umen JG. High-resolution profiling of a synchronized diurnal transcriptome from *Chlamydomonas reinhardtii* reveals continuous cell and metabolic differentiation. *Plant Cell*. 2015:27(10):2743–2769. https://doi.org/10.1105/tpc.15.00498

Zoschke R, Bock R. Chloroplast translation: structural and functional organization, operational control, and regulation. *Plant Cell*. 2018:30(4):745–770. https://doi.org/10.1105/tpc.18.00016